

# Supporting Information: Link between allosteric signal transduction and functional dynamics in a multi-subunit enzyme: S-adenosylhomocysteine hydrolase

Yoonji Lee,<sup>†</sup> Lak Shin Jeong,<sup>‡</sup> Sun Choi,<sup>\*,†</sup> and Changbong Hyeon<sup>\*,¶</sup>

*College of Pharmacy, Division of Life and Pharmaceutical Sciences, and National Core Research Center for Cell Signaling and Drug Discovery Research, Department of Bioinspired Sciences, Ewha Womans University, Seoul 120-750, and School of Computational Sciences, Korea Institute for Advanced Study, Seoul 130-722, Republic of Korea*

E-mail: sunchoi@ewha.ac.kr; hyeoncb@kias.re.kr

---

<sup>†</sup>Division of Life and Pharmaceutical Sciences, Ewha Womans University

<sup>‡</sup>Division of Life and Pharmaceutical Sciences, Department of Bioinspired Sciences, Ewha Womans University

<sup>¶</sup>Korea Institute for Advanced Study

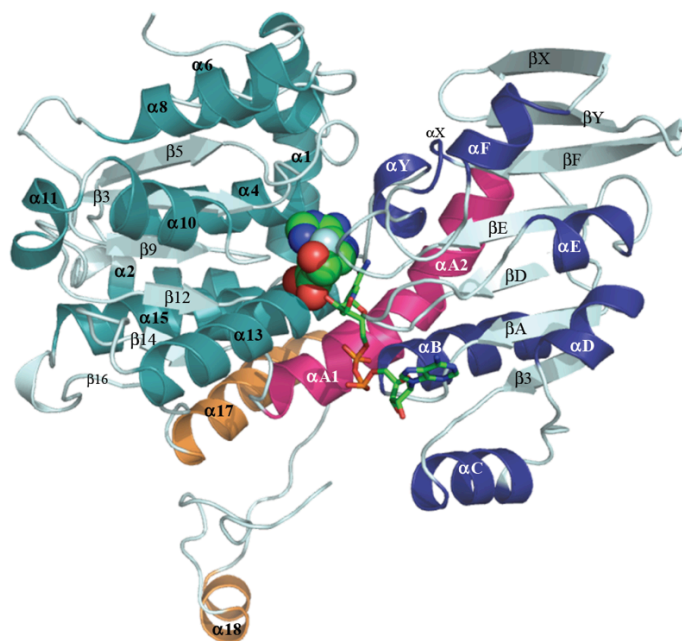


Figure S1: The secondary structural elements in SAH hydrolase. The alpha helices of the catalytic, cofactor-binding and C-terminal domains are colored by cyan, blue and orange, respectively, while those of the hinge region are in magenta. The beta sheets and loops are colored by light-blue. The nomenclatures of the structural motifs follow those in the study by Turner *et al.*<sup>1</sup>s:  $\alpha 1$ , 12-28;  $\alpha 2$ , 30-39;  $\beta 3$ , 49-53;  $\alpha 4$ , 58-69;  $\beta 5$ , 73-77;  $\alpha 6$ , 86-95;  $\beta 7$ , 99-101;  $\alpha 8$ , 107-118;  $\beta 9$ , 127-130;  $\alpha 10$ , 134-142;  $\alpha 11$ , 144-149;  $\beta 12$ , 152-155;  $\alpha 13$ , 158-170;  $\beta 14$ , 177-179;  $\alpha A1$ , 184-188;  $\alpha A2$ , 189-207;  $\beta A$ , 215-219;  $\alpha B$ , 223-234;  $\beta B$ , 238-242;  $\alpha C$ , 246-254;  $\beta C$ , 258-260;  $\alpha D$ , 262-268;  $\beta D$ , 271-274;  $\alpha E$ , 284-289;  $\beta E$ , 294-298;  $\alpha F$ , 308-314;  $\beta X$ , 315-322;  $\beta Y$ , 325-330;  $\beta F$ , 333-339;  $\alpha X$ , 340-342;  $\alpha Y$ , 345-349;  $\alpha 15$ , 355-374;  $\beta 16$ , 383-385;  $\alpha 17$ , 388-402;  $\alpha 18$ , 411-417.

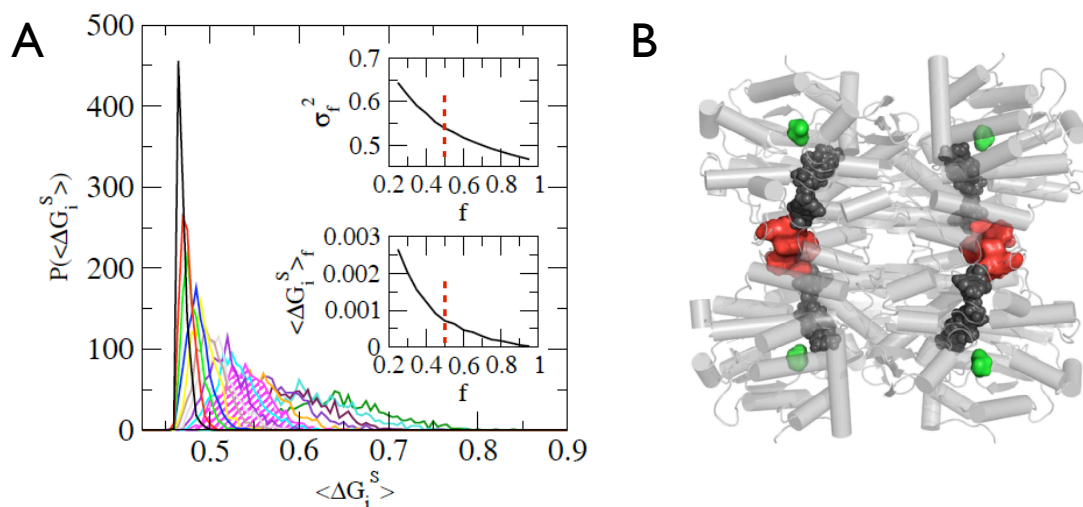


Figure S2: Results of statistical coupling analysis. **A.** Distribution of average free energy for sub-alignment,  $\langle G_i^s \rangle$ , for various sizes ( $N_s = f \times N_{MSA}$ ). **B.** Among SCA-identified hot-spot residues, highly conserved residues that satisfies  $\Delta G_i \geq 0.75$  are mainly found in the C-terminal domain and at C79. Green and red surfaces represent C79, and residues in C-terminal domain, respectively. Black spheres at each subunit represent the cofactor and ligand.

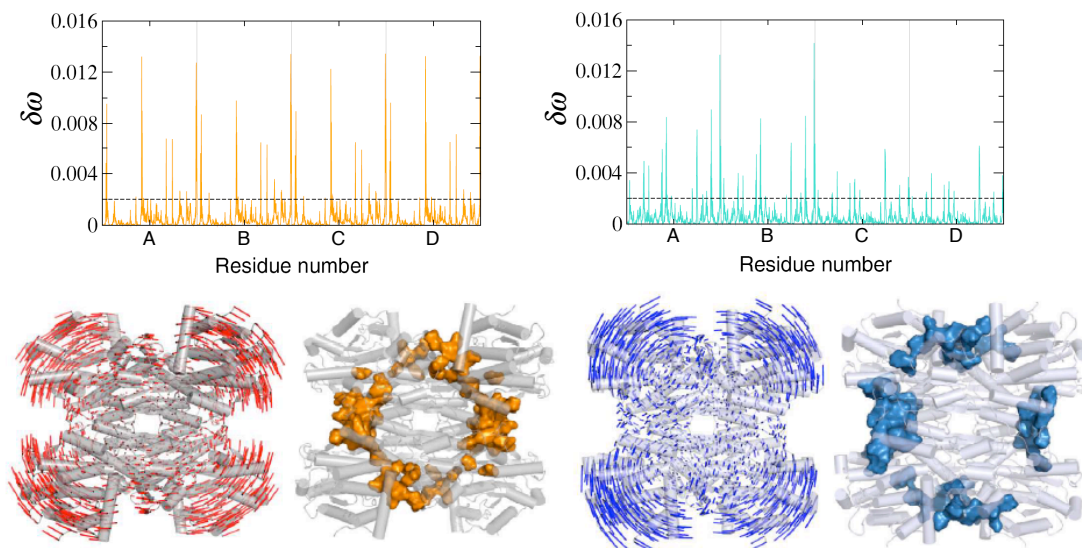


Figure S3: Results from structure perturbation method.  $\delta\omega$  values with respect to the next highly overlapping mode ( $\vec{v}_{M=9}$ ) with  $\vec{r}_{O \rightarrow C}$  for the open (orange) and closed (skyblue) forms (top). The  $\vec{v}_{M=9}$  for the open and closed forms are depicted on the structure with red and blue lines, respectively, and listed in the Table S2.

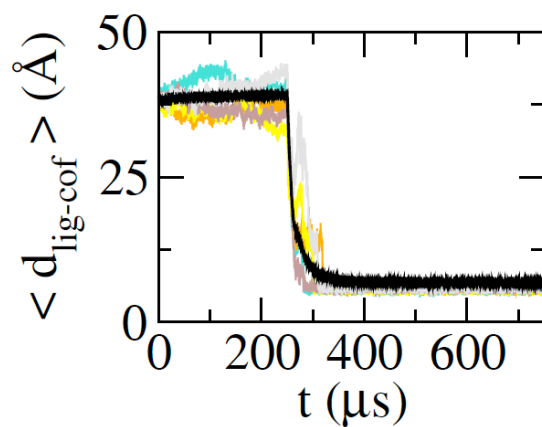


Figure S4: Ligand binding probed using the distance between the ligand and cofactor.

Open form (mode 7)				Closed form (mode 7)			
A chain	B chain	C chain	D chain	A chain	B chain	C chain	D chain
27	27	27	27	24	24	24	24
30	30	30	30				27
	32	32		166		166	166
	34	34				184	184
59	59	59	59		214	214	
*181	*181	*181	*181	215	215	215	215
*182	*182	*182	*182	238	238	238	238
*184	*184	*184	*184	246	246		246
	*185	*185	*185	257	257	257	257
	*186	*186		258	258	258	258
*187	*187	*187	*187	270	270	270	270
*188	*188	*188	*188	271	271		271
*190	*190	*190	*190	292	292	292	292
246			246	293	293	293	293
293			247	321	321	321	321
*354	*354	*354	*354	327	327	327	327
*355	*355	*355	*355	388	388	388	388
*358	*358	*358	*358	399	399	399	399
	361	361		401	401	401	401
367	367	367	367	403	403	403	403
	387	387		404	404	404	404
390	390	390	390	405	405	405	406
393	393	393	393	406	406	406	
	394	394	394	407	407	407	407
396	396	396	396	409	409		
397	397	397	397		418	418	418
399	399	399	399	421	421		421
401	401	401	401	424	424	424	424
402	402	402	402	427	427		
431	431	431	431			431	
432	432	432	432				

\*residues in the hinge region

Figure Table S1: The list of hot spot residues identified with SPM for the mode 7 in open and closed forms.

Open form (mode 9)				Closed form (mode 9)			
A chain	B chain	C chain	D chain	A chain	B chain	C chain	D chain
21	21	21	21	17	17	17	17
24	24	24	24	80	80	80	80
	25			82	82	82	82
	59	59		83	83		
156		156	156	104	104	104	104
*182	*182	*182	*182	162	162	162	162
*184	*184	*184	*184	165	165		
*185	*185	*185	*185	182	182	182	182
	*187			184	184	184	184
*190	*190	*190	*190	185			
*191		*191		187	187		
209			209	188	188		
223			223	206	206		
293	293	293	293	207	207	207	207
321	321	321	321	301	301		
	*353	*353		302	302		
	*354	*354		321	321	321	321
*355	*355	*355	*355	322	322	322	322
385	385	385	385	323	323	323	323
	387	387	387	324	324	324	324
	392			349	349		
428	428	428	428	350			
429	429	429	429	367	367		
430	430	430	430		368		
431	431	431	431	386	386	386	388
432	432	432	432	388	388	388	427
				390	390		
				427	427	427	
				428	428		
				430	430		
				431	431	431	431
				432	432		

\*residues in the hinge region

Figure Table S2: The list of hot spot residues identified with SPM for the mode 7 in open and closed forms.

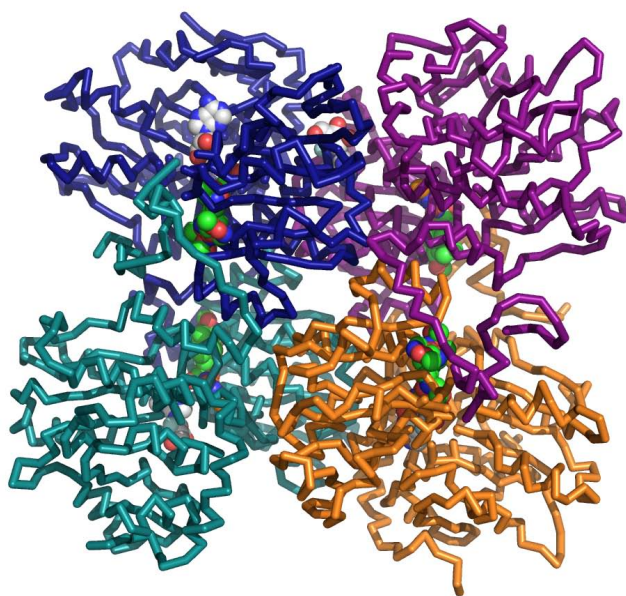


Figure Movie S1: A simulation of ligand-binding induced conformational change of SAHH.

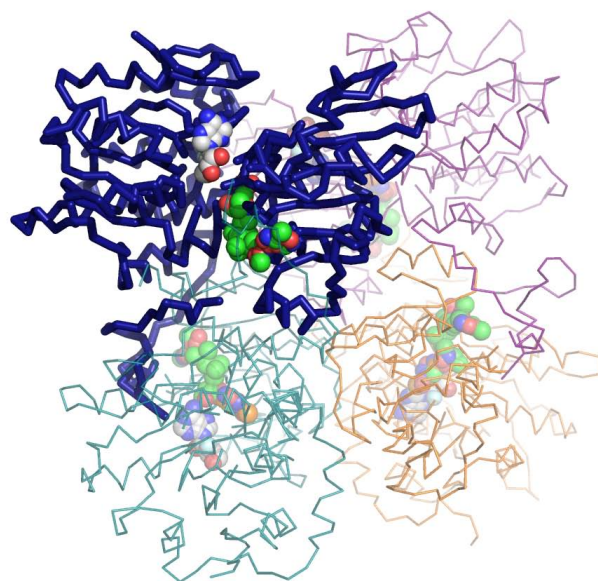


Figure Movie S2: A simulation of ligand-binding induced conformational change of SAHH, a cleft view



## References

- (1) Turner, M. A.; Yuan, C. S.; Borchardt, R. T.; Hershfield, M. S.; Smith, G. D.; Howell, P. L.  
*Nature Struct. Biol.* **1998**, *5*, 369–376.